

Experimental demonstration of tunable negative phase velocity and negative refraction in a ferromagnetic/ferroelectric composite metamaterial

Hongjie Zhao, Lei Kang, Ji Zhou, Qian Zhao, Longtu Li, Liang Peng, and Yang Bai

Citation: [Applied Physics Letters](#) **93**, 201106 (2008); doi: 10.1063/1.3033397

View online: <http://dx.doi.org/10.1063/1.3033397>

View Table of Contents: <http://scitation.aip.org/content/aip/journal/apl/93/20?ver=pdfcov>

Published by the [AIP Publishing](#)

Articles you may be interested in

[Ferromagnetic metamaterial with tunable negative index of refraction](#)

J. Appl. Phys. **107**, 013507 (2010); 10.1063/1.3275857

[Ferromagnetic resonance in ferromagnetic/ferroelectric Fe/Ba Ti O₃/Sr Ti O₃ \(001\)](#)

J. Appl. Phys. **103**, 07B108 (2008); 10.1063/1.2834243

[Ferroelectric-dielectric tunable composites](#)

J. Appl. Phys. **99**, 074104 (2006); 10.1063/1.2186004

[Tailoring of ferromagnetic Pr_{0.85}Ca_{0.15}MnO₃/ferroelectric Ba_{0.6}Sr_{0.4}TiO₃ superlattices for multiferroic properties](#)

Appl. Phys. Lett. **85**, 4424 (2004); 10.1063/1.1811800

[Theory of low-frequency magnetoelectric effects in ferromagnetic-ferroelectric layered composites](#)

J. Appl. Phys. **92**, 7681 (2002); 10.1063/1.1522834

The banner features a blue background with a molecular structure of spheres and rods. On the left is a thumbnail image of the 'Applied Physics Reviews' journal cover, which shows a diagram of a layered material. The text 'NEW Special Topic Sections' is prominently displayed in white. Below this, the text 'NOW ONLINE' is in orange, followed by 'Lithium Niobate Properties and Applications: Reviews of Emerging Trends' in white. The AIP Applied Physics Reviews logo is in the bottom right corner.

NEW Special Topic Sections

NOW ONLINE
Lithium Niobate Properties and Applications:
Reviews of Emerging Trends

AIP Applied Physics Reviews

Experimental demonstration of tunable negative phase velocity and negative refraction in a ferromagnetic/ferroelectric composite metamaterial

Hongjie Zhao,¹ Lei Kang,¹ Ji Zhou,^{1,a)} Qian Zhao,¹ Longtu Li,¹ Liang Peng,² and Yang Bai³

¹Department of Materials Science and Engineering, State Key Laboratory of New Ceramics and Fine Processing, Tsinghua University, Beijing 100084, People's Republic of China

²Electromagnetics Academy at Zhejiang University, Zhejiang University, Hangzhou 310027, People's Republic of China

³Corrosion and Protection Center, Key Laboratory of Environmental Fracture (Ministry of Education), University of Science and Technology Beijing, Beijing 100083, People's Republic of China

(Received 15 May 2008; accepted 28 October 2008; published online 20 November 2008)

A tunable left-handed transmission is demonstrated experimentally in a ferromagnetic/ferroelectric composite metamaterial (CMM) consisting of an array of yttrium iron garnet (YIG) rods combined with barium strontium titanate (BST) rods. We observed a passband in the CMM within the overlap of the stop bands of YIG rods alone and BST rods alone. Both measured phase velocity and refractive index of the CMM are shown to be negative at the relevant frequency range. The frequency showing left handedness can be adjusted continuously, dynamically, and reversibly by an applied magnetic field with a sensitive response of 3.5 GHz/kOe. © 2008 American Institute of Physics. [DOI: 10.1063/1.3033397]

Materials with simultaneously negative permittivity and negative permeability, i.e., left-handed materials (LHMs), have aroused great interest for their unique electromagnetic properties including negative phase velocity (NPV) and negative refraction (NR).¹⁻⁴ Since these exotic properties are not readily available in natural materials, much attention has been paid to metamaterials such as metallic wires² and split ring resonators (SRRs).³ As a result, most reported negative electromagnetic parameters of metamaterials originate from the structures rather than from the materials. Hence, it would be interesting and significant to design LHMs using all dielectrics (all-DEs)⁵⁻¹² such as proposed DE spherical particle,⁶⁻⁹ disk,^{10,11} and rod.¹² Within these DEs, a strong electric response is determined by their electric parameters (ϵ_r). A strong magnetic response excited by a displacement current loop, however, is not determined naturally by their magnetic parameters (μ_r). In this letter, we demonstrate experimentally tunable NPV and NR in an all-DE composite metamaterial (CMM) consisting of an array of ferromagnetic (FM)/ferroelectric (FE) ceramic rods. In our all-DE CMM, the strong magnetic response is excited by FM resonance (FMR) of the FM ceramic, which naturally originates from the interaction between spin magnetic dipoles and dynamic magnetic field.

Considering a CMM of FM/FE thin rods (inset of Fig. 1) with $\lambda > 5d$, where λ is the characteristic wavelength, we can regard the CMM as a homogeneous medium with an effective permeability $\mu_{\text{eff}}^{\text{CMM}}$ and effective permittivity $\epsilon_{\text{eff}}^{\text{CMM}}$. For the magnetic excitation mode shown in inset of Fig. 1, $\mu_{\text{eff}}^{\text{CMM}}$ can be derived as¹³

$$\mu_{\text{eff}}^{\text{CMM}}(\omega) = 1 - \frac{\eta F \omega_{\text{mp}}^2}{\omega^2 - \omega_{\text{mp}}^2 - i\Gamma(\omega)\omega}, \quad (1)$$

where $\eta = a/d$ is a fraction of the FM rods interacted with dynamic magnetic field \mathbf{H}_{rf} . Definitions of other parameters in Eq. (1) are referred to Ref. 13. Further calculation under $\mathbf{H}_0 = 2200$ Oe, $4\pi M_s = 1700$ G, $\alpha = 0.003$, $a = 0.8$ mm, and $d = 5$ mm reveals negative $\mu_{\text{eff}}^{\text{CMM}}$ from 10.36 to 10.78 GHz (Fig. 1). The shape (rod) choice of the FM unit cell is based on two considerations. First, it requires a smaller \mathbf{H}_0 , compared with other shapes, to excite FMR at the same frequency due to static demagnetization;¹⁴ second, it ensures a two-dimensional (2D) isotropy in xoy plane due to the 2D isotropic dynamic demagnetization in the cross section. For electric excitation mode shown in Fig. 1, if the FE cylinders have a high DE constant ϵ_r^{FE} , an electric resonance along z axis can be set up within the FE rod.¹² Considering $\epsilon_{\text{eff}}^{\text{FE}}$ of the

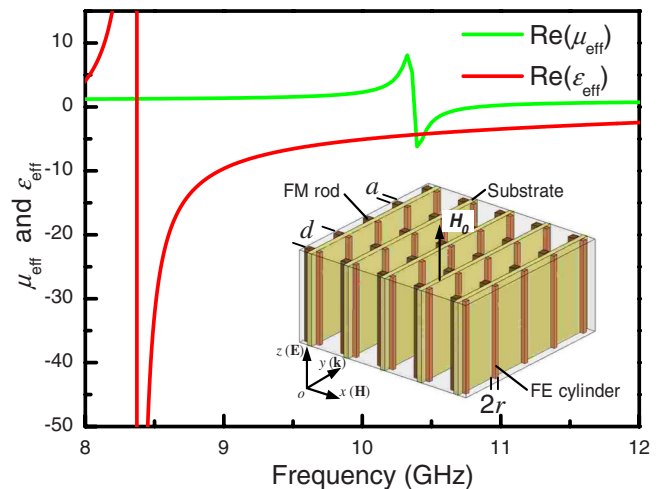


FIG. 1. (Color online) Calculated effective permeability and permittivity for CMM consisting of an array of FM rods and FE cylinders. Inset shows schematic of the rectangular slab of the CMM.

^{a)} Author to whom correspondence should be addressed. Electronic mail: zhouji@mails.tsinghua.edu.cn.

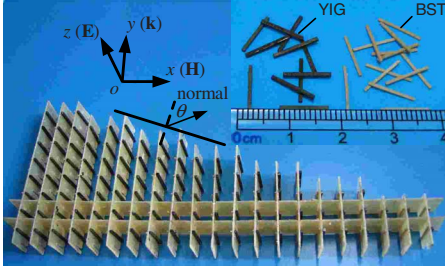


FIG. 2. (Color online) Photograph of prism of the CMM consisting of YIG rods and BST rods. Inset shows photograph of the YIG rods and BST rods.

FE cylinders alone¹² and ϵ_r^{FM} of the FM rods alone, we can express $\epsilon_{\text{eff}}^{\text{CMM}}$ approximately as

$$\epsilon_{\text{eff}}^{\text{CMM}}(\omega) = \frac{(1 - \xi)(R^2 - r^2)}{R^2} [1 + I_e(r, R)] + \xi \epsilon_r^{\text{FM}}, \quad (2)$$

where $\xi = (a/d)^2$ is a fraction of the FM rods interacted with dynamic electric field \mathbf{E}_{rf} , r is a radius of the FE cylinder, $R = d/\sqrt{\pi}$ is an integral radius corresponding to d , and $I_e(r, R)$ is a function of ϵ_r^{FE} and the cylinder's dimension. Further calculation under $\epsilon_r^{\text{FE}} = 850$, $\epsilon_r^{\text{FM}} = 14.3$, $r = 0.3$ mm, $a = 0.8$ mm, and $d = 5$ mm reveals negative $\epsilon_{\text{eff}}^{\text{CMM}}$ from 8.4 to 12 GHz (Fig. 1).

For FM medium, polycrystalline rods of yttrium iron garnet (YIG) are commercially available with a size of $0.8 \times 0.8 \times 10.0$ mm³, saturation magnetization of $4\pi M_s = 1700$ G, DE constant of $\epsilon_r^{\text{YIG}} = 14.3$, and resonance linewidth of $\Delta H = 12$ Oe. For FE medium, rods of barium strontium titanate (BST) with a composition of $\text{Ba}_{0.5}\text{Sr}_{0.5}\text{TiO}_3$ doped with 5 wt % MgO are prepared by solid-phase reaction, tape casting technique, and sintering processing. Final BST rods have a size of $0.5 \times 0.5 \times 10.0$ mm³ and microwave DE constant of $\epsilon_r^{\text{BST}} = 850 \pm 20$ estimated with the frequency of first Mie resonance for cut BST cubes. The two kinds of rods are pasted on both sides of a 0.6 mm thick FR-4 substrate ($\epsilon = 4.4$ and $\tan \delta = 0.014$). For one-dimensional transmission and phase measurements performed by a waveguide WR90, the unit cells are assembled into rectangular slabs of CMMs with various cells along y axis (N_y) and fixed cells along x axis ($N_x = 5$), as shown in inset of Fig. 1. The lattice constants are $d = 5$ mm. For refraction measurements performed by a setup similar to that in Ref. 4, a prism of CMM is constructed with $d = 6$ mm (Fig. 2). The minimum and maximum numbers of unit cells at the propagation direction are 2 and 8, respectively, which result in a wedge angle of 18.4° . For the refraction measurement, the setup needs to be checked beforehand with a Teflon prism. Both measurements are carried out by a network analyzer HP8720ES under different applied magnetic fields \mathbf{H}_0 , which are provided by an electromagnet along z axis. A microwave propagates along y axis with \mathbf{E}_{rf} parallel to z axis and \mathbf{H}_{rf} parallel to x axis.

Transmissions (S_{21}) through sole BST rods, sole YIG rods, and the rectangular slab of CMM with $N_x = N_y = 5$ were measured under $\mathbf{H}_0 = 2340$ Oe and shown in Fig. 3(a). It can be seen that the YIG rod array exhibits a band gap between 10.7 and 10.8 GHz, while the BST rod array exhibits a wide stop band between 9.3 and 12 GHz. The band gap of YIG resulted from FMR, hence the effective permeability is negative for this gap, while the stop band of BST resulted from

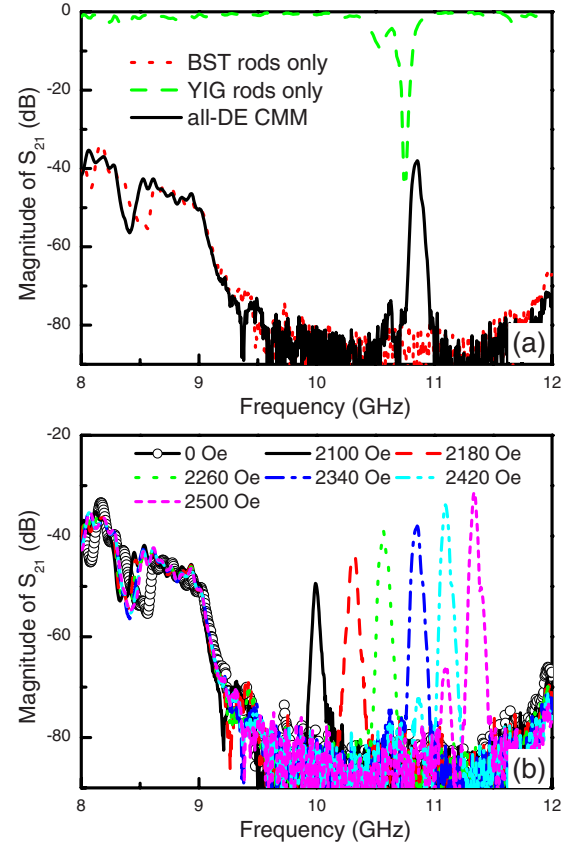


FIG. 3. (Color online) (a) Measured transmission spectra for sole BST rods, sole YIG rods, and rectangular slab of the CMM under $\mathbf{H}_0 = 2200$ Oe. (b) Measured transmission spectra for the CMM slab under different applied magnetic fields.

electric resonance, hence the effective permittivity is also negative for this gap. By combining the YIG rods with the BST rods to form the CMM, we observed a transmitted passband just within the overlap of the stop bands of the YIG alone and the BST alone. Furthermore, the passband measured under different \mathbf{H}_0 reveals its magnetically tunable property, as shown in Fig. 3(b) where the passband frequency increases from 9.95 to 11.35 GHz as \mathbf{H}_0 rises from 2100 to 2500 Oe with a sensitive response of 3.5 GHz/kOe. As \mathbf{H}_0 decreases the passband frequency decreases and, after removing \mathbf{H}_0 , the transmission spectrum returns to its original zero-field state, i.e., the passband disappears (data are not shown here), indicating continuity and reversibility of the tuning. The tunability of the passband frequency is attributed to that of the band gap frequency of the YIG rods, which increases/decreases as \mathbf{H}_0 increases/decreases. The disappearance of the passband after removing \mathbf{H}_0 resulted from the negligible remanence of YIG. Moreover, a similar tunable passband can also be observed in rotated slab of the rectangular CMM on z axis for $\pi/2$ (data are not shown here), which reveals a 2D isotropy of the passband. The 2D isotropy is attributed to the fact that the dynamic magnetization on the YIG rods meets an isotropic demagnetization within xoy plane.

By measurements of transmitted phases and refractive angles, we demonstrated the left handedness of the passband of the CMM. An unwrapped transmitted phase will help us verify whether a passband is LH.^{15,16} The transmitted phase of the rectangular slab with various N_y was measured under $\mathbf{H}_0 = 2340$ Oe to investigate the phase velocity within the

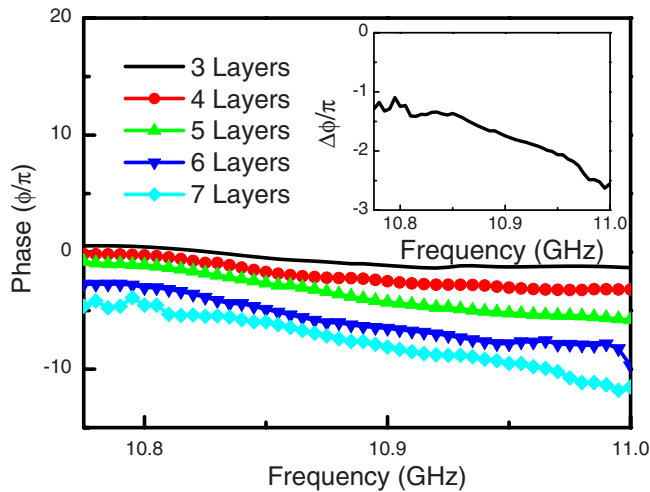


FIG. 4. (Color online) Unwrapped transmitted phase obtained from different lengths of the CMM slab between 10.77 and 11.00 GHz under $\mathbf{H}_0 = 2340$ Oe, where LH transmitted peak takes place. Inset shows average phase difference between consecutive numbers of layers of CMM.

passband. As shown in Fig. 4, the phase decreases as N_y increases, which implies a typical LH behavior. As shown in the inset of Fig. 4, average phase shifts $\Delta\Phi$ are negative for the relevant frequency range, indicating a NPV.

NR in wedge structures is a typical experimental method used for observation of LH properties in CMMs. The angular refraction spectrum is scanned in the prism of the FM/FE CMM by a step of 2.5° , while the frequency is swept from 10 to 12 GHz under $\mathbf{H}_0 = 2500$ Oe. Figure 5 shows the transmitted power as a function of frequency and of angle from the normal. It is evident that the transmitted beam is refracted on the negative side from the normal. The maximum power occurs at $\theta = -30^\circ$ for 11.36 GHz. To investigate the beam profile, the angular cross section at 11.36 GHz is plotted in the inset of Fig. 5. By employing Snell's law the refractive index can be defined for the CMM as $n = -1.58$.

In conclusion, we have demonstrated a tunable 2D LH transmission in an all-DE CMM consisting of FM/FE ceramic rods within microwave region. We experimentally confirmed a NPV and a NR in the transmitted passband for the all-DE CMM. Response of the magnetically tuning for the LH transmission is achieved averagely with 3.5 GHz/kOe. Compared to the previous LHMs based on tunable metallic SRRs, the presented all-DE LHM based on FM/FE CMM opened a promising realm for designing tunable LHMs with a broader tuning range, a more sensitive response, and a smaller scale, provided proper FM/FE ceramics and applied fields are concerned. Furthermore, a ceramic

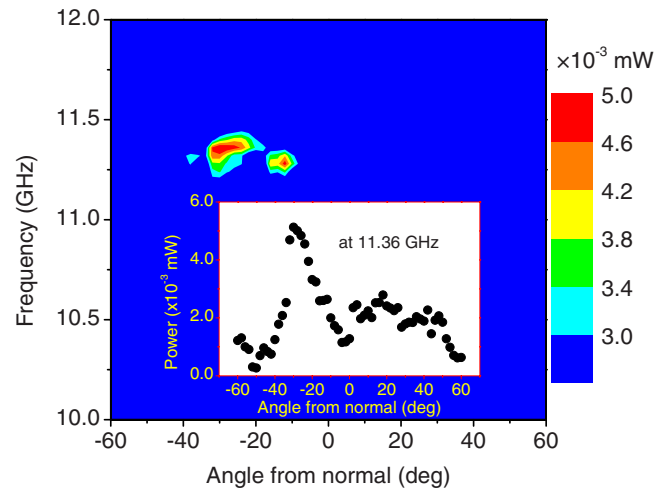


FIG. 5. (Color online) Measured transmitted power as a function of frequency and of angle from the normal. Inset shows the angular cross section of the transmitted beam at 11.36 GHz.

cofiring technique could make the mentioned CMM homogeneous magnetoelectric composite, which would be promising to design subwavelength devices for terahertz.

This work is supported by the National Science Foundation of China under Grant Nos. 50425204, 50572043, 50632030, 50621201, and 10774087.

- ¹V. G. Veselago, *Sov. Phys. Usp.* **10**, 509 (1968).
- ²J. B. Pendry, A. J. Holden, W. J. Stewart, and I. Youngs, *Phys. Rev. Lett.* **76**, 4773 (1996).
- ³J. B. Pendry, A. J. Holden, D. J. Robbins, and W. J. Stewart, *IEEE Trans. Microwave Theory Tech.* **47**, 2075 (1999).
- ⁴R. A. Shelby, D. R. Smith, and S. Schultz, *Science* **292**, 77 (2001).
- ⁵A. L. Efros and A. L. Pokrovsky, *Solid State Commun.* **129**, 643 (2004).
- ⁶C. L. Holloway, E. F. Kuester, J. Baker-Jarvis, and P. Kabos, *IEEE Trans. Antennas Propag.* **51**, 2596 (2003).
- ⁷I. Vendik, O. Vendik, and M. Odit, *Microw. Opt. Technol. Lett.* **48**, 2553 (2006).
- ⁸L. Jylhä, I. Kolmakov, S. Maslovski, and S. Tretyakov, *J. Appl. Phys.* **99**, 043102 (2006).
- ⁹V. Yannopapas and A. Moroz, *J. Phys.: Condens. Matter* **17**, 3717 (2005).
- ¹⁰T. Ueda, A. Lai, and T. Itoh, *IEEE Trans. Microwave Theory Tech.* **55**, 1280 (2007).
- ¹¹E. A. Semouchkina, G. B. Semouchkin, M. Lanagan, and C. A. Randall, *IEEE Trans. Microwave Theory Tech.* **53**, 1477 (2005).
- ¹²L. Peng, L. Ran, H. Chen, H. Zhang, J. A. Kong, and T. M. Grzegorzczuk, *Phys. Rev. Lett.* **98**, 157403 (2007).
- ¹³H. Zhao, J. Zhou, Q. Zhao, B. Li, L. Kang, and Y. Bai, *Appl. Phys. Lett.* **91**, 131107 (2007).
- ¹⁴B. Lax and K. J. Button, *Microwave Ferrites and Ferrimagnetics* (McGraw-Hill, New York, 1962), Vol. 304, p.7.
- ¹⁵K. Aydin, K. Guven, C. M. Soukoulis, and E. Ozbay, *Appl. Phys. Lett.* **86**, 124102 (2005).
- ¹⁶K. Aydin, Z. Li, L. Sahin, and E. Ozbay, *Opt. Express* **16**, 8835 (2008).